4402–4416 *Nucleic Acids Research, 2008, Vol. 36, No. 13* *Published online 2 July 2008*
doi:10.1093/nar/gkn413

Physical and functional characterization of the genetic locus of IBtk, an inhibitor of Bruton's tyrosine kinase: evidence for three protein isoforms of IBtk

Carmen Spatuzza[1], Marco Schiavone[1], Emanuela Di Salle[2], Elzbieta Janda[1], Marco Sardiello[3], Giuseppe Fiume[1], Olga Fierro[4], Marco Simonetta[2], Notis Argiriou[2], Raffaella Faraonio[2], Rosanna Capparelli[5], Ileana Quinto[1,*] and Giuseppe Scala[1]

[1]Department of Experimental and Clinical Medicine, University of Catanzaro 'Magna Graecia', 88100 Catanzaro, [2]Department of Biochemistry and Medical Biotechnology, University of Naples 'Federico II', [3]Telethon Institute of Genetics and Medicine, 80131 Naples, [4]Institute of Food Sciences, CNR, Avellino and [5]Department of Biotechnological Sciences, University of Naples 'Federico II', Naples, Italy

Received January 9, 2008; Revised June 12, 2008; Accepted June 13, 2008

ABSTRACT

Bruton's tyrosine kinase (Btk) is required for B-cell development. Btk deficiency causes X-linked agammaglobulinemia (XLA) in humans and X-linked immunodeficiency (Xid) in mice. Btk lacks a negative regulatory domain and may rely on cytoplasmic proteins to regulate its activity. Consistently, we identified an inhibitor of Btk, IBtk, which binds to the PH domain of Btk and down-regulates the Btk kinase activity. IBtk is an evolutionary conserved protein encoded by a single genomic sequence at 6q14.1 cytogenetic location, a region of recurrent chromosomal aberrations in lymphoproliferative disorders; however, the physical and functional organization of *IBTK* is unknown. Here, we report that the human *IBTK* locus includes three distinct mRNAs arising from complete intron splicing, an additional polyadenylation signal and a second transcription start site that utilizes a specific ATG for protein translation. By northern blot, 5′RACE and 3′RACE we identified three *IBTKα*, *IBTKβ* and *IBTKγ* mRNAs, whose transcription is driven by two distinct promoter regions; the corresponding IBtk proteins were detected in human cells and mouse tissues by specific antibodies. These results provide the first characterization of the human *IBTK* locus and may assist in understanding the *in vivo* function of IBtk.

INTRODUCTION

Bruton's tyrosine kinase (Btk) is a member of the Tec family of nonreceptor protein tyrosine kinases that includes TECI and TECII, BMX, TXK, ITK and Dsrc 28C (1–3). These kinases are characterized by the Src homology-1 (SH1) tyrosine kinase domain and by additional SH2 and SH3 regions, which function as protein–protein interaction sites (4). The structure of Btk includes a unique NH_2-terminal region containing a Plecktrin homology (PH) domain that regulates the Btk kinase activity; accordingly, mutations in several *BTK* domains lead to a severe X-linked agammaglobulinemia (XLA) in humans (5). Moreover, a specific mutation of the conserved Arg^{28} residue in the Btk-PH domain leads to a severe X-linked immunodeficiency (Xid) phenotype in mice (6,7). Individuals with XLA show a severe immunodeficiency as a consequence of a significant reduction of mature B cells and immunoglobulin levels (4). Accordingly, mice with Xid carry mutations in the *BTK* gene and show a decreased number of mature B cells that fail to proliferate properly upon B-cell receptor (BCR) cross-linking (4,8). Several signal pathways are induced upon Btk kinase activation. Evidence from Btk-deficient B cells (DT40) (9) indicates that Btk is required for a proper tyrosine phosphorylation of phospholipase C-gamma (PLC-γ), which in turn leads to inositol-3,4,5-triphosphate (IP_3), a major mediator of $[Ca^{2+}]$i mobilization, and to diacylglycerol, an activator of protein kinase C (PKC) (10,11). These pathways activate specific transcription factors, including nuclear

*To whom correspondence should be addressed. Tel: +39 0961 3694058 (office); Fax: +39 0961 3694090; Email: quinto@unicz.it
Correspondence may also be addressed to Giuseppe Scala. Tel: +39 0961 3694059 (office); Fax: +39 0961 3694090; Email: scala@unicz.it
Present address:
Notis Argiriou, Center for Research and Technology-Hellas, 570 01 Thermi–Thessaloniki, Greece

The authors wish it to be known that, in their opinion, the first three authors should be regarded as joint First Authors

factor-kappaB (NF-κB) and BAP135-TFII-I (12–15), which regulate the gene transcription program required for B-cell survival and cell-cycle progression. Btk activation is also induced upon a direct interaction between the Btk-PH domain and G-protein subunits (16). Further, Btk regulates some intracellular apoptotic pathways and plays a role in cell-cycle regulation and tumorigenesis of B cells (9,17,18). Indeed, Btk is a major regulator of B-cell apoptosis and cooperates with tumor suppressor genes, including SLP-65 (17–20).

Little is known of the regulation of Btk function. Unlike Src proteins, Btk lacks a negative regulatory domain and may rely on cytoplasmic Btk-binding proteins to regulate its kinase activity by *trans*-inhibitor mechanisms. Consistent with this possibility, we have studied a newly identified inhibitor of Btk (IBtk), which binds specifically to the PH domain of Btk and down-regulates its kinase activity. IBtk was isolated by screening a human B-lymphoblastoid cDNA library in the yeast two-hybrid system by using specific domains of Btk as a bait (21). The results were as follows: (i) IBtk is an evolutionary conserved protein encoded by a single genomic sequence at a 6q14.1 cytogenetic location, a region of recurrent chromosomal aberrations in lymphoproliferative disorders (22,23); (ii) IBtk specifically associates with Btk, as demonstrated by both *in vitro* and *in vivo* protein–protein interaction assays. Confocal microscopy revealed a submembrane co-localization of IBtk and Btk and (iii) upon binding to Btk, IBtk down-regulates the Btk kinase activity, as shown by using as a substrate both endogenous Btk and a peptide corresponding to the Btk-SH3 domain that includes the Tyr223 autophosphorylation site (21). Btk is essential for B-cell survival and cell-cycle progression following BCR triggering (4,24,25). In this setting, Btk regulates $[Ca^{2+}]$i entry and mobilization from intracellular stores that ultimately lead to the activation of transcription factors, including NF-κB (12,14). Consistent with the above results, IBtk inhibited the $[Ca^{2+}]$i fluxes in Indo-1-loaded DT40 cells upon anti-IgM stimulation and the NF-κB-driven transcription was observed upon anti-IgM stimulation; IBtk expression resulted in a dose-dependent inhibition of this activity (21). These results indicate that IBtk plays a crucial role in the *in vivo* regulation of Btk-mediated B-cell function; however, no reports have addressed the physical and functional characterization of the *IBTK* locus. In this study, we report a detailed description of the human *IBTK* locus and provide evidence for a complex genomic organization that gives rise to three distinct mRNAs, *IBTKα*, *IBTKβ* and *IBTKγ*, which are translated in the corresponding proteins IBtkα, IBtkβ and IBtkγ.

MATERIALS AND METHODS

Genomic analysis of the *IBTK* genomic locus

Canis familiaris, *Bos taurus*, *Mus musculus*, *Gallus gallus*, *Xenopus tropicalis*, *Fugu rubripes* and *Tetraodon nigroviridis* genomic sequences were searched for *IBTK* homologous genes with TBLASTN (http://www.ncbi.nih.gov/BLAST/) and BLAT (http://genome.ucsc.edu/) using the amino acid sequence of human IBtkα as a query. The retrieved genomic segments were aligned to the available cDNA/EST sequences to infer the gene architecture. For genes that lacked a transcript counterpart, a careful manual examination of candidate genomic sequences was performed, by looking for splicing donor and acceptor signals to define the gene structure (26,27).

Evolutionary analysis of *IBTK* gene

Amino acid sequence alignments were performed with MULTIALIN (28). Local evolution rates over the amino acid sequences of IBtkα proteins were estimated with the evolution–structure–function method (29). This analysis requires a preliminary reconstruction of the evolutionary relationships among all analyzed peptides. We built the phylogenetic tree of investigated IBtkα proteins using PHYLO-WIN (30) and by holding its branching pattern constant, we calculated the number of substitution per site in each 15-residue wide window over the entire amino acid alignment with CODEML (31). Finally, rate values were calculated by dividing the number of substitutions per site in each window by the average of all windows (providing the 'relative rate'). The final values were then computed by smoothing the relative rates with a seven-position moving window arithmetic average. The evolutionary profile was plotted as a function of alignment position in a 2D array. A ranked list of local minima, which define the evolutionarily constrained regions (ECRs), was obtained by scanning the array from the bottom (minimum) to top (maximum). Pair-wise sequence identities were calculated at the European Bioinformatics Institute website (http://www.ebi.ac.uk/emboss/align/). Synonymous and nonsynonymous substitution ratios were calculated at the SNAP website [http://www.hiv.lanl.gov; (32)]. Analysis of canonical and noncanonical splice sites in mammalian genomes was performed as reported (33) by mining GenBank, EMBL (34), and UCSC Genome Browser Database (35).

IBTK intron 24 amplification from *Pongo pygmaeus* and *Pan troglodytes*

Genomic DNA of *P. pygmaeus* and *P. troglodytes* were used to test the evolutionary conservation of *IBTK* intron 24 among the primate nonhuman species. Genomic DNA (250 ng) was used to perform a PCR reaction. Specific primers were used to amplify the *IBTK* intron 24: primer ex24f (5′-GTC AGC CCT CCT GTT GTG GAT-3′) and primer ex25r (5′-TGC ATT CAC TGG TTT GGG GGC-3′). The amplified DNA was eluted from the agarose gel and analyzed by sequencing with an ABI PRISM DNA sequencing system (Applied Biosystems, Foster City, CA, USA).

Cell cultures

MC3 and DeFew B cells (36), NB4 and Jurkat T cells were grown in RPMI 1640 (Cambrex, East Rutherford, NJ, USA) supplemented with 10% fetal bovine serum (FBS) (Cambrex), 2mM L-glutamine, 100 U/ml of penicillin and 100 U/ml of streptomycin (Biowhittaker, Walkersville, MD, USA). 293T (human embryonic kidney cells) and HeLa (human epithelial cells from cervical carcinoma)

cells were grown in DMEM (Cambrex) containing 10% FBS, 2mM L-glutamine, 100 U/ml of penicillin and 100 U/ml of streptomycin. Cell lines were incubated at 37°C with 100% humidity in 5% CO_2. Peripheral blood mononuclear cells (PBMC) were isolated from buffy coats by using Ficoll Paque gradient (GE Healthcare Europe, Munich, Germany). Briefly, donor blood was diluted 1:10 in PBS 1× and stratified on Ficoll solution with a 3:1 v/v ratio. After a 30 min centrifugation at 2200 r.p.m., PBMC were recovered and re-suspended in RPMI-1640 medium supplemented with 10% FCS.

RNA extraction and RT–PCR

Total RNA was extracted by using the TRIzol reagent (Invitrogen, Karlsruhe, Germany). PolyA mRNA was isolated by using Oligotex mRNA Mini Kit (Qiagen, Hilden, Germany). MC3 total RNA (200 ng) and polyA mRNA (20 ng) was used to synthesize three double strand cDNAs with SuperScript One-Step RT–PCR with Platinum Taq (Invitrogen). Briefly, the RT–PCR reactions were performed in a single step using three pairs of *IBtkα*, *IBtkβ*, *IBtkγ* specific primers: (i) ex24f (5′-GTC AGC CCT CCT GTT GTG GAT-3′) coupled with I24r (5′-TGG ATC AAA ATG CTC ACA AGT T-3′) amplified a cDNA fragment of *IBtkβ*; (ii) ex24f (5′-GTC AGC CCT CCT GTT GTG GAT-3′) coupled with ex25r (5′-TGC ATT CAC TGG TTT GGG GGC-3′) amplified a cDNA fragment of *IBtkα* and (iii) I24f (5′-TGG GCA ATT TAG CCT CCA TA-3′) coupled with ex25r (5′-TGC ATT CAC TGG TTT GGG GGC-3′) amplified a cDNA fragment of *IBtkγ*. The cDNA fragments were analyzed by electrophoresis on 1.5% agarose gel and sequenced.

Northern blot

MC3, Jurkat and HeLa polyA mRNA (1 μg) was fractionated by electrophoresis on a formaldehyde–1% agarose gel and transferred on Hybond N^+ nylon strips (GE Healthcare). Filters were alternatively hybridized with two ^{32}P-labeled human *IBTK* fragments: ex12 probe and int24 probe. A ^{32}[P]-labeled human GAPDH fragment was used as equal loading control probe. The following primers were used to generate DNA amplicons as probes: for *IBTK* (α and β) ex12 probe: ex12f 5′-GCA ATA GAC TCT TCC CTG CAC-3′ and ex12r 5′-GGC AGA AGA GCA AAC CTA AAT-3′; for *IBTKγ* int24 probe: I24/f 5′-TGG GCA ATT TAG CCT CCA TA-3′ and I24r 5′-AAC TTG TGA GCA TTT TGA TCC A-3′; for *GAPDH* probe: GAPDHf 5′-GAA GGT GAA GGT CGG AGTC-3′, GAPDHr: 5′-GAA GAT GGT GAT GGG ATT TC-3′.

5′-rapid amplification of cDNA end

PolyA mRNA was isolated from MC3 cells by using the TRIzol reagent method (Invitrogen) and Oligotex mRNA mini kit (Qiagen). Two 5′-rapid amplification of cDNA end (5′RACE) reactions were performed by using 5′RACE System 2.0 kit (Invitrogen) to find two transcription start sites (TSS): one for *IBTKα* and *IBTKβ*, and a distinct one for *IBTKγ*. The 5′RACE was performed in three reactions: one RT–PCR to synthesize the first strand cDNA followed by two nested PCR. Briefly, the first strand cDNAs were synthesized from 1 μg of mRNA by SuperScriptII RNA polymerase reaction using the specific primers GSP1R (5′-GAG TGA GGA GGG GAA CT-3′) for *IBTKα* and *IBTKβ*, and GSP6R (5′-GAG TCA AGT TTC TGG GAT GTA ATA CTG-3′) for *IBTKγ*. After adding an oligo-dC tail to the 3′-ends of cDNAs, two nested PCR rounds were performed using more internal primers. The first nested PCR round was performed with GSP2R primer (5′-GGT GAC CAG TCG CTA GAT GAA A-3′), specific for *IBTKα* and *IBTKβ* and GSP5R primer (5′-GAG TCA AGT TTC TGG GAT GTA ATA CTG-3′) specific for the *IBTKγ*, coupled with an Abridged Anchor Primer (AAP) (5′-GGC CAC GCG TCG ACT AGT ACG GGI IGG GII GGG IIG-3′) containing oligo-dI-dG at the 3′-end of the primer. The second nested PCR round was performed with GSP3R primer (5′-GGT GGA TTC CGC AGG GTC CAC ATA-3′) specific for *IBTKα* and *IBTKβ* and GSP4R primer (5′-GGA GGC TAA ATT GCC CAG AAA AGG-3′) specific for *IBTKγ*. The resulting DNA fragments were eluted from agarose gel and were analyzed by sequencing with an ABI PRISM DNA sequencing system (Applied Biosystems).

3′-rapid amplification of cDNA end

To map the 3′-end of the three transcripts *IBTKα*, *IBTKβ* and *IBTKγ*, we performed two 3′-rapid amplification of cDNA end (3′RACE) reactions. The first strand cDNAs were synthesized from 1 μg of MC3 PolyA mRNA by reverse transcriptase using 3′RACE System (Invitrogen) with a 3′RACE primer displaying an adaptor sequence at the 5′-end of the oligo-dT (5′-GGC CAC GCG TCG ACT AGT ACT TTT TTT TTT TTT TTT T-3′). Three PCR-rounds were performed: in the first one, cDNA was amplified with the adaptor primer and specific primers, GSP4L (5′-CCT TTT CTG GGC AAT TTA GCC TCC ATA-3′) for *IBTKβ* and GSP7L (5′-GCC TGG GAG ACA CAT AAG CAA T-3′) for *IBTKα* and *IBTKγ*. The first nested PCR round was performed by using adaptor primer and other more internal specific primers, GSP5L (5′-CAG TAT TAC ATC CCA GAA ACT TGA CTC-3′) for *IBTKβ* and GSP8L (5′-GAA GGT AAG CCT GGG AGA CAC ATA -3′) for *IBTKα* and *IBTKγ*. The last nested PCR round was performed by using adaptor primer and specific primers GSP6L (5′-GTG ATA TGT TGG AGG GCT CAT A-3′) for *IBTKβ* and GSP9L (5′-CAG AAG TTC TCT GAA CCT CAA TTG T-3′) for *IBTKα* and *IBTKγ*. Following electrophoresis in 2% agarose gel, the final PCR product was eluted (QIAEXII Gel Extraction kit—Qiagen). DNA sequence was determined with an ABI PRISM DNA sequencing system (Applied Biosystems).

IBTK-luciferase reporter assays

Distinct fragments of *IBtkα*, *IBtkβ* and *IBtkγ* promoter regions were obtained by PCR amplification of human genomic DNA and inserted in pGL3-basic vector (Promega, Madison, WI, USA) after digestion with KpnI and BglII. For *IBtkα* and *IBtkβ* promoter, we analyzed four fragments designed as: −754/+22, −159/+22,

−82/+22 and −67/+22. The following forward primers were used: for −754/+22, 5′-GGG GTA CCA GGC ATT CAG CAG CAG TGT G-3′; for −159/+22, 5′-GGG GTA CCC GGC GAG GTC AAG TTC CTT T-3′; for −82/+22, 5′-GGG GTA CCG CAC CAG CCA ATC ATC AAG AG-3′; for −67/+22, 5′-GGG GTA CCC AAG AGA CAT ACA GGA GCC C-3′. The reverse primer was: 5′-GAA GAT CTC GGG AAC GGG GAT GTA GA-3′. In the case of the *IBTKγ* promoter, we analyzed two fragments designed as: −691/+5 and −155/+5. The following forward primers were used: for −691/+5, 5′-GGG GTA CCG GCT GTA GTG CAG TGG TAT GAT-3′; for −155/+5, 5′-GGG GTA CCT CCT GTC AGC CCT CCT GTT G-3′. The reverse primer was: 5′-GAA GAT CTG TCT GTC CAA TTC TTA GGG CAG AA-3′.

Cell transfection and luciferase reporter assays were performed as follows: 293T cells (3×10^5/well) were seeded in 6-well tissue culture plates 24 h before transfection. Cells were transfected by using the calcium phosphate method (Invitrogen) according to the manufacturer's instruction. The luciferase gene expression driven by an empty pGL3 Basic vector was used as negative control. To normalize the transfection efficiency, cells were co-transfected with pCMV β-gal vector (0.2 μg), which expresses the *β-galactosidase* gene from the cytomegalovirus promoter (Clontech, Mountain View, CA, USA). Each sample was transfected with *luc* reporter plasmids (0.5 μg). Twenty-four hours posttransfection, cells were washed twice with PBS and harvested. Cell lysates and luciferase reporter assay were performed using Dual Light System (Applied Biosystem). Results were normalized according to the luciferase to β-galactosidase activity ratio and normalized for the protein concentration. A minimum of four independent experiments were performed; arithmetic mean and SEM values were used for graphic representation.

Real-time PCR analysis

Real-time quantitative RT–PCR on *IBTK* cDNAs was carried out with the iQ™ SYBR® Green Super mix using the iCycler iQ real-time detection system (Bio-Rad, Munich, Germany) with the following conditions: 95°C, 1 min; (94°C, 10 s; 60°C, 30 s) × 40. The oligonucleotides for PCR were RT24f (5′-CCTCCTGTTGTGGATCTC AGAACTAT-3′) and RT25r (5′-GAGAAAGTTTAAC TCCATGAGAAAC-3′) for *IBTKα*; RT24f and RT24Ar (5′-AGGGCAGAAATACAACATGAAATG-3′) for *IBTKβ*; RT24If (5′-CCAGTAACCTTTATTAAGCAG AAATTAATGTTA-3′) and RT25rII (5′-CATGCATTC ACTGGTTTGGGGGC-3′) for *IBTKγ*. The reactions were performed in triplicate using as templates cDNA preparations from 15 different human tissues [Human multiple tissue cDNA (MTC) Panel I and II, Clontech] and the following cell types: HeLa, DeFew, Jurkat cell lines and primary PBMC. Expression levels were calculated relative to *GAPDH* mRNA levels as endogenous control. Relative expression was calculated as $2^{(\text{Ct test gene} - \text{Ct GAPDH})}$ (37). Oligo efficiencies were tested using as a template serial dilutions of α, β and γ amplicons cloned in pTA cloning vector plasmid (Invitrogen).

IBtk antibodies production and western blot analysis

Antibody against IBtkα and IBtkβ was raised in chicken by taking advantage of a unique peptide sequence, NFHEDDNQKS, not shared by the *G. gallus* (shown in Figure S1). Two chickens were immunized with 31B peptide NFHEDDNQKSC (aa 672–681 of IBtkα and IBtkβ) conjugated with KLH (keyhole limpet hemocyanin) (Gallus Immunotech Inc., Fergus, ON, Canada). One primary immunization (0.75 mg of 31B peptide in Freund's complete adjuvant) and three boostings (0.25 mg of 31B peptide in Freund's incomplete adjuvant) were performed. IgY anti-31B specific were purified by affinity chromatography using 31B-conjugated sepharose (NHS-activated Sepharose 4 Fast Flow, GE Healthcare). In addition, to overcome the constraint of amino acid sequence homology of IBtk over multiple species, including *M. musculus*, polyclonal antibodies against IBtkα and IBtkγ were raised in *Ibtk*$^{-/-}$ mouse by GST-IBtkγ immunization. The development of the *Ibtk*$^{-/-}$ mouse will be reported elsewhere. The cDNA fragment corresponding to the full-length IBtkγ was generated by RT–PCR (Invitrogen) of total RNA isolated from MC3 cells, by using the following primers: 5′-CGGAATTCCGGTGGTGGTGGTCCGTTAATTGA TATAATTTCTAGCAAAATGATTTCTC-3′ and 5′-CC GCTCGAGGCATCTCAACTCCACAGTG-3′. The fragment was inserted in pGEX-4T-3 vector (GE Healthcare) at EcoRI and XhoI sites. GST-IBtkγ protein was expressed in BL21 host *Escherichia coli* strain. Insoluble GST-IBtkγ was recovered from inclusion bodies by using a denaturing solution (8 M urea, 1% Triton X-100, 5 mM DTT) and purified by gel electrophoresis. Mice were primed with 0.2 mg of GST-IBtkγ in Freund's complete adjuvant and boosted with three distinct inoculations of GST-IBtkγ (0.1 mg) in incomplete Freund's adjuvant. The titers and specificity of anti-IBtk sera were assessed by ELISA. Endogenous IBtk proteins were detected by western blot as follows: mouse (adult C57BL) and human cells were lyzed in RIPA buffer (50 mM Tris–HCl pH 7.4, 1% NP-40, 150 mM NaCl, 1 mM EDTA, 1 mM PMSF and protease inhibitors) and subjected to SDS–polyacrylamide 8% or 12% gel electrophoresis followed by transfer to a PVDF membrane (GE Healthcare). IBtkα and IBtkβ were detected by using the chicken 31B IgY antibody (10 μg/ml) followed by incubation with a anti-chicken-HRP (Gallus Immunotech Inc.). The binding specificity was assessed by preincubating the primary antibody with the 31B peptide (molar ratio IgY/peptide = 1/1000). IBtkα and IBtkγ proteins were detected by using an anti-GST-IBtkγ serum (dilution 1:500) followed by incubation with anti-mouse-HRP (GE Healthcare). In the case of DeFew cells, the primary antibody was preincubated with either GST (60 nmoles/ml), or GST-IBtkγ (60 nmoles/ml). Cellular γ-tubulin was detected by immunoblotting with a specific antibody (Sigma-Aldrich, Buchs, SG, Switzerland) followed by an anti-mouse-HRP (GE Healthcare). Antibody–protein bindings were visualized by enhanced chemiluminescence (ECL and ECL Plus, GE Healthcare).

Regulation of *IBTK* transcripts by an *IBTK*-specific shRNA

HEK 293 LinX packaging cell line (Open Biosystem, Huntsville, AL, USA) was cultured in DMEM containing 10% FBS, 2 mM L-glutamine, 100 U/ml of penicillin and 100 U/ml of streptomycin 100 µg/ml of hygromycin. Jurkat cells expressing either a stably control shRNA, or the *IBTK*-shRNA SH2407H3, were cultured in RPMI-1640 supplemented with 10% FBS, 2 mM L-glutamine, 100 U/ml of penicillin, 100 U/ml of streptomycin and 1 µg/ml puromycin. HEK 293 LinX packaging cell line (Open Biosystem) was transfected with 10 µg of either empty plasmid, or with a plasmid expressing the IBTK-specific shRNA clone SH2407H3 (Open Biosystem). Forty-eight hours posttransfection, the cell supernatants were collected and filtered with 0.45 µm. Jurkat cells (4×10^6) were infected with 1 ml of filtered supernatant by spinoculation (38); 24 h later, the culture medium was supplemented with 1 µg/ml puromycin. The sequence of IBTK shRNA SH2407H3 was 5′-TGCTGTTGACAG TGAGCGACGGGATTTCTTACTAGAAGAATAGTG AAGCCACAGATGTA**TTCTTCTAGTAAGAAATCCC GG**TGCCTACTGCCTCGGA-3′ with annealing sequence to exon 26 of the *IBTKα* transcript (nucleotide +4162–4183; shown in bold). The shRNA sequence is also specific for the *IBTKγ* transcript (nucleotide +692–713); shown in Figure S6B.

Protein–protein interaction

PBMC extracts were performed in RIPA-Buffer. Antibodies (5 µg) were preincubated with (20 µl) of protein G-Agarose (GammaBind Plus Sepharose GE Healthcare) in 200 µl of immunoprecipitation RIPA buffer overnight at 4°C on a rocking platform. The cell extracts were precleared on protein G. The protein G-agarose-coupled antibodies were incubated with cell extract (1 mg) in 500 µl of immunoprecipitation RIPA buffer overnight at 4°C on a rocking platform. The immunocomplexes were collected by centrifugation at 2200 r.p.m. for 3 min at 4°C, washed five times in 900 µl of RIPA buffer and resuspended in SDS gel loading buffer. The proteins were separated on either 8% or 12% SDS–polyacrylamide gel, transferred to PVDF membrane and analyzed by immunoblotting. IBtkα and IBtkβ were detected by using the chicken 31B IgY antibody (10 µg/ml) followed by incubation with a anti-chicken-HRP (Gallus Immunotech Inc.). IBtkγ was detected by using an anti-GST-IBtkγ serum (dilution 1:500) followed by incubation with anti-mouse-HRP (GE Healthcare). The following antibodies were used for immunoprecipitation and for control immunoblotting: anti-Btk (E-9), anti-Emt (Itk) (2F12), anti-PLCγ1 (E-12) and anti-Akt1 (B-1), normal mouse IgG1 (Santa Cruz, Santa Cruz, CA, USA).

Confocal analysis

Intracellular localization of IBtk isoforms in B lymphoma cells (DeFew) was assessed by confocal microscopy as previously described (21,39). The cDNA fragments corresponding to the full-length IBtkα, IBtkβ and IBtkγ were generated by RT–PCR (Invitrogen) of total RNA isolated from MC3 cells, by using the following primers: for IBtkα 5′-CCGAAGCTTCCTGACTGCACATCAAAGT GTCGATC-3′ and 5′-CGGGATCCCTAGCATCCAT GCTTATTCAACATAGG-3′, for IBtkβ 5′-CCGAAG CTTCCTGACTGCACATCAAAGTGTCGATC-3′ and 5′-CGGGATCCGAGTCAAGTTTCTGGGATGTAAT ACTG-3′, for IBtkγ 5′-TTAATTGATATAATTTCTAG CAAAATGATTTCTC-3′ and 5′-CGGGATCCCTAGC ATCCATGCTTATTCAACATAGG-3′. The fragment was inserted in p3XFLAG-CMV-7.1 vector (Sigma) at HindIII and BamH1 sites. DeFew cells were transiently transfected with plasmids coding for the three isoforms of IBtk (α, β and γ) fused to FLAG tag. Twenty-four hours later the cells were fixed and stained with FITC-conjugated anti-FLAG Ab (Green) and anti-Btk Ab, followed by Alexa-568 secondary Ab (Red, Molecular Probes, Eugene, OR, USA) and DAPI to detect nuclear DNA. DeFew B cells were seeded on poly-L-lysine-treated glass coverslips, fixed and permeabilized using Cytofix/CytoPerm kit (BD Biosciences Pharmingen, San Diego, CA, USA). Coverslips were mounted on glass slides by using ProLong Antifade Kit (P7481, Molecular Probes). Images were collected on a Leica TCS-SP2 confocal microscope (Leica Mycrosystems, Wetzlar, Germany) with a 63× Apo PLA oil immersion objective (NA 1.4) and 60 µm aperture. Z stacks of images were collected using a step increment of 0.2 µm between planes. In each panel, a single plane confocal image shows the center of a transfected cell (Figure 7).

RESULTS

Bioinformatic analysis of the *IBTK* genomic locus

The *IBTK* locus was mapped at the 6q14.1 cytogenetic location (21). We took advantage of the annotated sequence of chromosome 6 (40) to compare the cDNA coding for *IBTK* with the putative gene present in region 6q14.1. This region reports a gene, termed *IBTK* according to the sequence accession number AL050333, which spans over a 77.576 kb genomic region and includes 29 putative exons (Figure 1A), with a predicted fully spliced mRNA of 5798 nucleotides (Figure 1B) with an ORF coding for a protein of 1353 amino acids with a MW of 150.53 kDa (Figure 1E; the amino acid sequence is shown in Figure S1A); this genomic sequence will be hereafter referred to as *IBTKα* (Figure 1B). A sequence analysis of the full-length *IBTK* sequence revealed a putative TSS within exon 1 and a polyadenylation signal (AAUAAA) within intron 24, which would give rise to a 4437 nucleotide mRNA (Figure 1C). This region includes an ATG translation start codon and a TAA stop codon with an ORF coding for a protein of 1196 amino acids with a MW of 133.87 kDa (Figure 1E; the predicted amino acid sequence is shown in Figure S1B); this putative transcript will be hereafter referred to as *IBTKβ* (Figure 1C).

The previously reported *IBTK* cDNA (21) (accession number: AF235049) is 2328-bp long and includes an ORF coding for a protein of 240 aa with a MW of 26.31 kDa. This cDNA shows a perfect match with fully spliced exons 25–29 of the *IBTK* gene and includes an additional nucleotide sequence located within intron

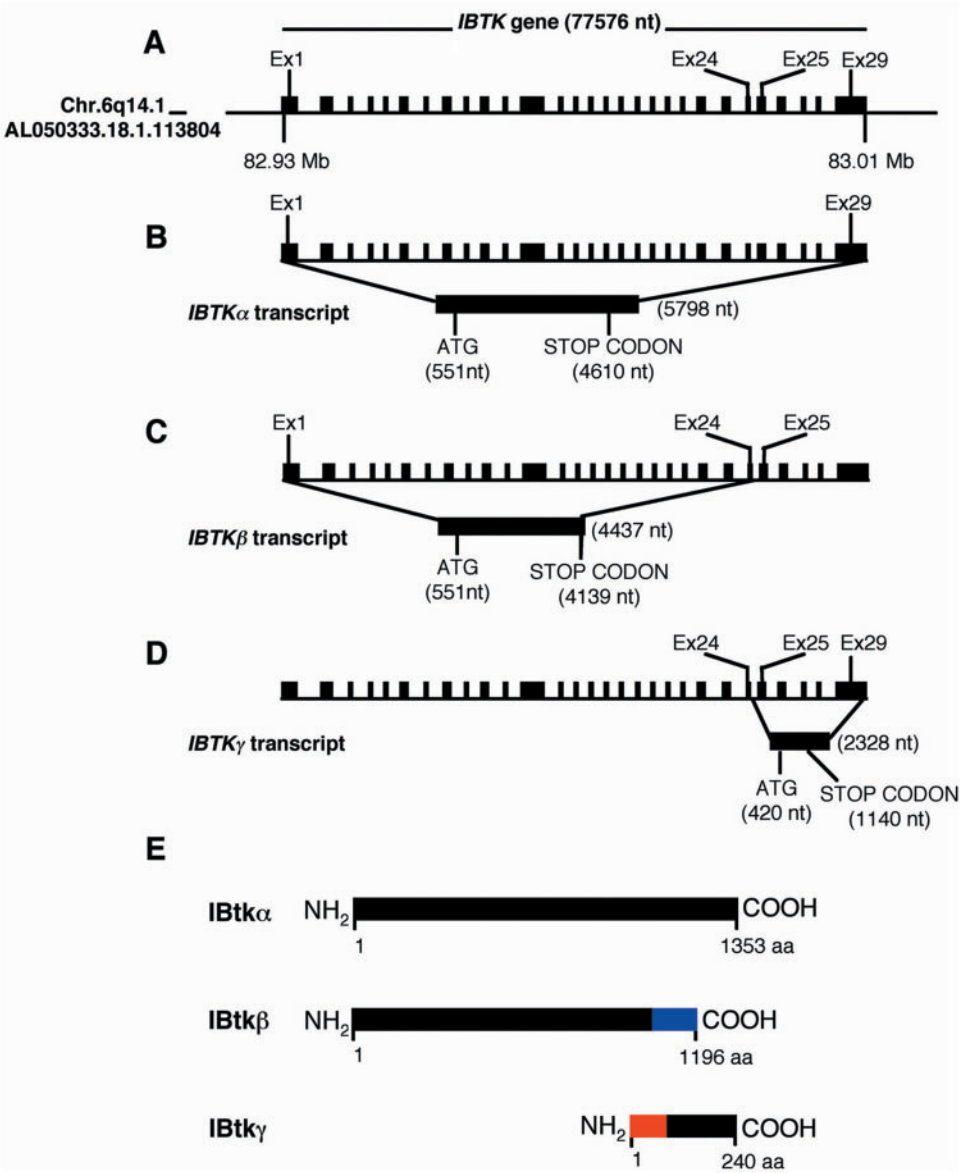

Figure 1. Schematic representation of the predicted *IBTK* mRNA and IBtk protein isoforms. (**A**) Schematic representation of the *IBTK* gene. The black bars depict the 29 exons of the gene. The numbers indicate the gene coordinates. (**B–D**) Representation of the predicted *IBTK* transcripts; the exons that contribute to the distinct transcripts are indicated as bold bars. Parenthetical number indicates the transcript length. The predicted ORFs of the distinct IBtk isoforms are indicated by the start and stop codons. **(E)** Schematic representation of the predicted IBtk protein isoforms (α, β and γ). Amino acid regions highlighted in blue (IBtkβ) or in red (IBtkγ) represent regions coded for the predicted additional exon located within intron 24.

24 of the *IBTKα* sequence (Figure 1D), which codes for 31 amino acids of the amino terminus of the protein, hereafter referred to as Ibtkγ (Figure 1E; the amino acid sequence is reported in Figure S1C).

Analysis of *IBTK* transcripts

According to bioinformatics analysis, northern blot of total RNA from HeLa, Jurkat and MC3 cells using specific probes was consistent with the occurrence of three distinct spliced RNAs leading to *IBTK* transcripts of about 6.0, 4.5 and 2.2 kb (Figure 2A).

To verify the occurrence of additional nucleotide sequences from intron 24 in *IBTK* transcripts, mRNA was isolated from MC3 cells followed by RT–PCR amplification and nucleotide sequencing. Primer pairs were selected according to the predicted *IBTK* transcripts (reported under Materials and methods section). Figure 2B shows a schematic representation of the region covering exons 24–25; this region includes intron 24, which hosts a putative TSS and a polyadenylation signal. The results of the RT–PCR analysis were as follows: (i) a fully spliced *IBTKα* RNA transcript, including the splicing of intron 24 (Figure 2C); (ii) a second *IBTKβ* transcript that originates from an RNA splicing of introns 1–23 and is terminated at a polyadenylation signal within intron 24 of the *IBTK* gene sequence (Figure 2D);

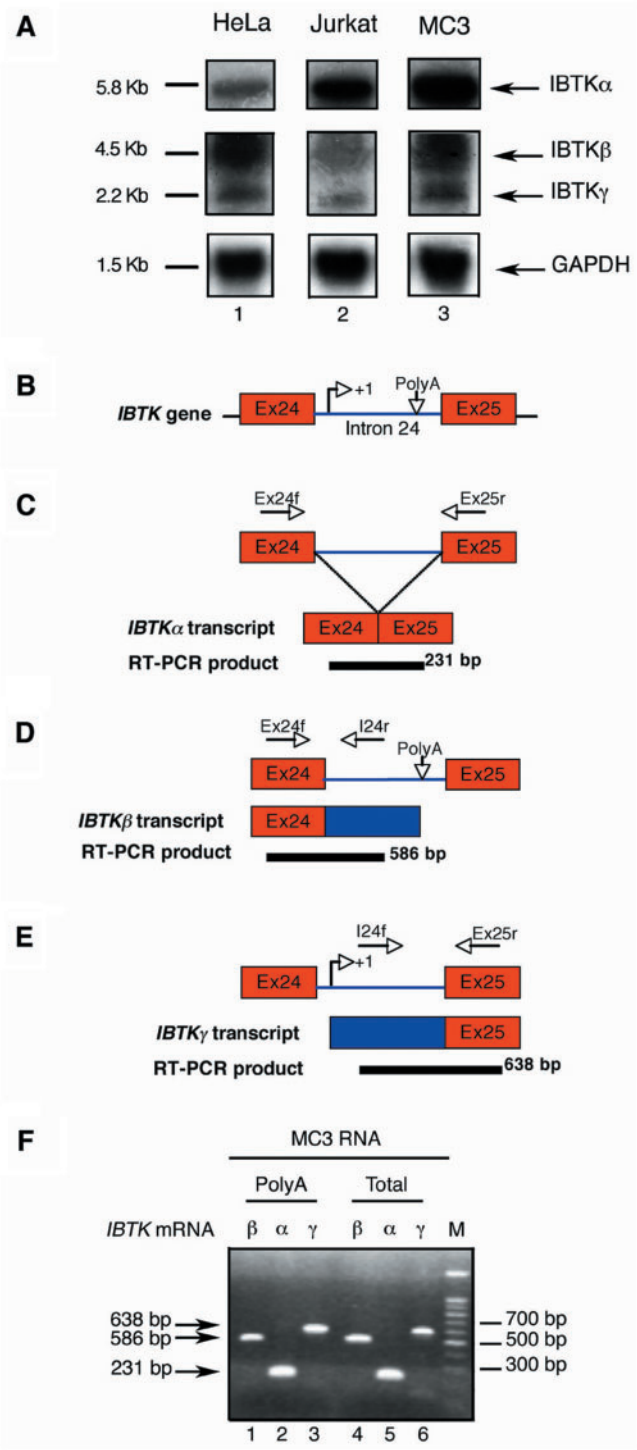

Figure 2. Analysis of *IBTK* transcripts. (**A**) Northern blot analysis of the distinct *IBTK* mRNAs in HeLa, Jurkat and MC3 cells as follows: (i) *IBTKα*, 5798 nt; (ii) *IBTKβ*, 4437 nt and (iii) *IBTKγ*, 2328 nt. (**B**) Schematic representation of the *IBTK* genomic region covering exons 24 and 25. The region of intron 24 reports the +1 nucleotide of *IBTKγ* transcript and the polyadenylation signal of *IBTKβ* transcript. (**C**) The splicing of intron 24 was assessed by RT–PCR analysis and nucleotide sequencing of the region of exons 24 and 25. The bold bar shows the length of the PCR product. (**D**) Schematic representation of the *IBTKβ* transcript that includes exon 24 and intron 24, as assessed by RT–PCR analysis of the *IBTK* region. The bold bar shows the length of the PCR product. The polyadenylation site identified within intron 24 is shown. (**E**) The *IBTKγ* transcript was identified by using specific primers as shown. The bold bar shows the length of the PCR product. The picture also includes the +1 nucleotide TSS as identified by 5′ RACE. (**F**) RT–PCR products of *IBTK* transcripts using the primers shown in (C–E).

(iii) a third *IBTKγ* transcript that originates from a TSS located within intron 24 (Figure 2E). The PCR-amplified transcripts are shown in Figure 2F.

Next, we identified the TSSs of the putative *IBTK* transcripts by using the 5′RACE. Both the *IBTKα* and *IBTKβ* transcripts originated from a +1 nucleotide (CTTCCTC) within exon 1, which was followed by an ATG translational start codon at nucleotide +551 (Figure S2A, left panel). In the case of the *IBTKγ* transcript, the TSS (CAGACT) was identified within intron 24 (Figure S2A, left panel). The 5′RACE products are shown in Figure S2A, right panel. Further, we performed a 3′RACE analysis of polyA mRNA to define the 3′-end three *IBTK* transcripts. The 3′RACE followed by PCR analysis and nucleotide sequencing confirmed the presence of one polyadenylation site shared by *IBTKα* and *IBTKγ* transcripts (Figure S2B, left panel) and a distinct polyadenylation site of the *IBTKβ* transcript within intron 24 (Figure 3B, left panel). The 3′RACE amplicons are shown in Figure S2B, right panel.

As summarized in Figure S2C, these results confirmed the occurrence of three distinct *IBTK* transcripts: (i) *IBTKα* mRNA (5798 nt) that arises from splicing of the complete set of 28 introns and represents the full-length *IBTKα* mRNA (sequence submission: DQ005633); (ii) *IBTKβ* mRNA (4437 nt) that is contributed by exons 1–24 and includes an additional region of 51 amino acids located within intron 24; this transcript results from the usage of a polyadenylation signal (AAUAAA) within intron 24 (sequence submission DQ005634). In this context, intron 24 is not spliced and functions as an extension of exon 24; (iii) *IBTKγ* mRNA (2328 nt) that includes a cap region within intron 24, which contributes a short exon that hosts a +1 TSS and codes for 31 amino acids of the amino terminus of IBtkγ protein (sequence submission: DQ005635).

Evolutionary analysis of the *IBTK* gene

To investigate whether similar *IBTKβ* and *IBTKγ* transcripts were present in other organisms related to humans, we performed a comparative analysis of human the *IBTK* intron 24 with the corresponding sequences from close and distant mammalian species. To this end, we amplified genomic DNA from chimp *P. troglodytes* and orang *P. pygmaeus* by PCR using primers flanking human *IBTK* intron 24 (Ex24f 5′-GTCAGCCCTCCTGTTGTG GAT-3′ and Ex25r 5′-TGCATTCACTGGTTTGGG GGC-3′). The PCR products were purified from agarose gels and sequenced (Figure S3). This analysis indicated that the distinct IBtk isoforms are conserved across different organisms. Indeed, we observed a 99% similarity across the analyzed species and a predicted production of the three IBtk protein isoforms (Figure S3). Further, we searched the mouse, cow and dog genomes for *IBTK* orthologs in BLAST analysis at the University of

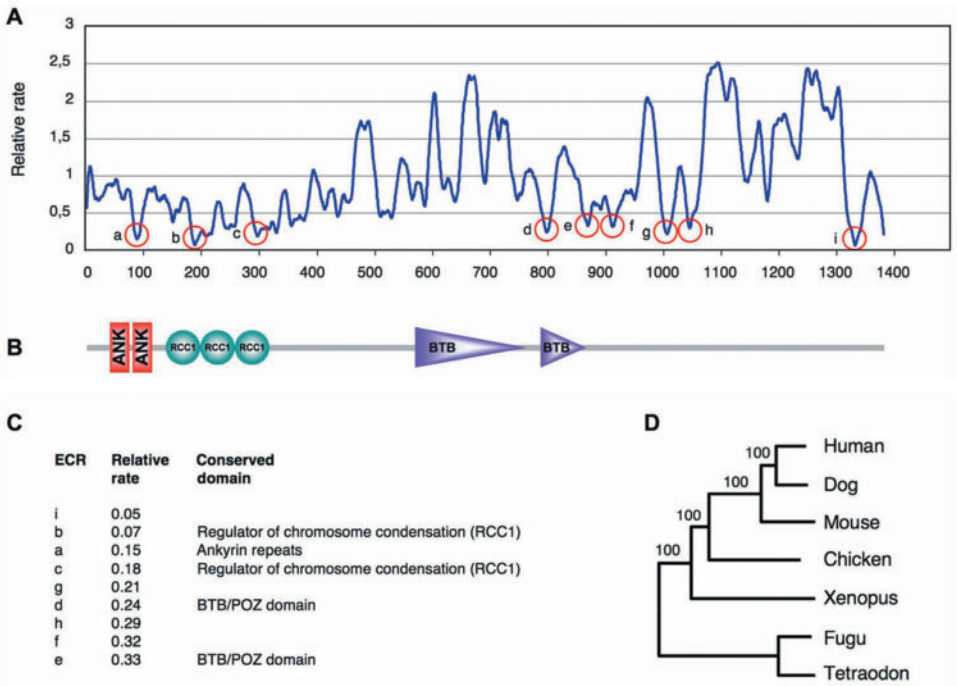

Figure 3. Evolutionary analysis of IBtk. (**A**) The diagram shows a plot of local evolutionary rates across vertebrate IBtk proteins from *H. sapiens*, *C. familiaris*, *M. musculus*, *G. gallus*, *X. tropicalis*, *F. rubripes* and *T. nigroviridis*. The values plotted on the *y*-axis are a measure of the average number of amino acid substitutions per site for residues at the corresponding *x*-axis position of the protein alignment. The red circles mark the nine highest scoring ECRs detected (ECRs A to I from N- to C-terminus). (**B**) Schematic of known protein domains found along the IBtk sequence. ANK, ankyrin repeats; RCC1, regulator of chromosome condensation; BTB, BTB/POZ domain. (**C**) A list of the detected ECRs is shown, which were ranked by their evolutionary relative rates. The correspondence between ECRs and known protein domains is shown. (**D**) Phylogenetic analysis of IBtk proteins. The enrooted maximum parsimony tree was used as an input for ECR analysis.

California at Santa Cruz (UCSC) genome browser by using the human sequence as a probe. Each retrieved sequence was carefully compared to the human *IBTK* genomic sequence using pair-wise TBLAST and TBLASTX, looking for splicing donor and acceptor sites to infer the gene architecture. The results showed that each investigated species has only one gene homologous to human *IBTK*. All genes share a common intron/exon structure (data not shown) and are therefore putative orthologs. The comparison of human *IBTK* intron 24 with its orthologous sequences showed that *P. pygmaeus*, *C. familiaris and B. taurus* have translation start codons ORFs that are contiguous to the downstream exons, as is the case of the human gene, indicating that their genomes can code for IBtkγ isoform (Figure S4). *Pongo pygmaeus, C. familiaris and B. taurus* also have the potential to encode an IBtkβ isoform (Figure S4). Conversely, all the potential start codons within the mouse *Ibtk* intron 24 are followed by stop codons; in this setting, IBtkγ isoform begins from an ATG codon located within exon 25 (Figure S4). In addition, the sequence analysis of mouse intron 24 showed a lack of the polyadenylation signal, suggesting that the IBtkβ protein isoform is not expressed in mice (Figure S4) (41). An investigation of rat *Ibtk* showed an analogous sequence configuration (data not shown).

The degree of evolutionary conservation for protein-coding regions and the rates of synonymous or nonsynonymous substitutions for the four investigated mammalian species (*H. sapiens*, *M. musculus*, *B. taurus* and *C. familiaris*) were calculated, and reported as Supplementary Figure S5. Sequence comparisons among the putative *IBTK* coding sequences in four species (*H. sapiens*, *M. musculus*, *B. taurus* and *C. familiaris*) showed that the *IBTKα*, *IBTKβ*, and *IBTKγ* isoforms do not differ significantly in terms of sequence conservation or evolutionary pressure (Figure S5).

Within a protein, sequences of functional relevance are subject to evolutionary constraints that force them to evolve with a significantly lower rate than other protein sites. Therefore, assessing ECRs can help to infer important functional sites along the protein sequence (29). To perform an ECR analysis of IBtkα, we retrieved additional homologous sequences from representative vertebrates (Chicken, Xenopus, Fugu and Tetraodon) at the UCSC genome browser (Figure 3). ECR analysis identified nine regions with strong conservation among all IBtkα protein (ECRs a–i) (Figure 3). A search of the PROSITE (42) and SMART (43) databases revealed that five ECRs fall within known protein domains: (i) Ankyrin repeats, which are short, tandemly repeated modules usually involved in protein–protein interaction (44,45); (ii) regulator of chromosome condensation 1 (RCC1), found in proteins that exert a role in the epigenetic modulation of gene expression (46,47) and (iii) BTB/POZ, found in transcriptional regulators that control chromatin structure (48,49) (Figure 3B and C). Conversely, no known protein domains could be assigned to some ECRs, including ECRi, which is the most

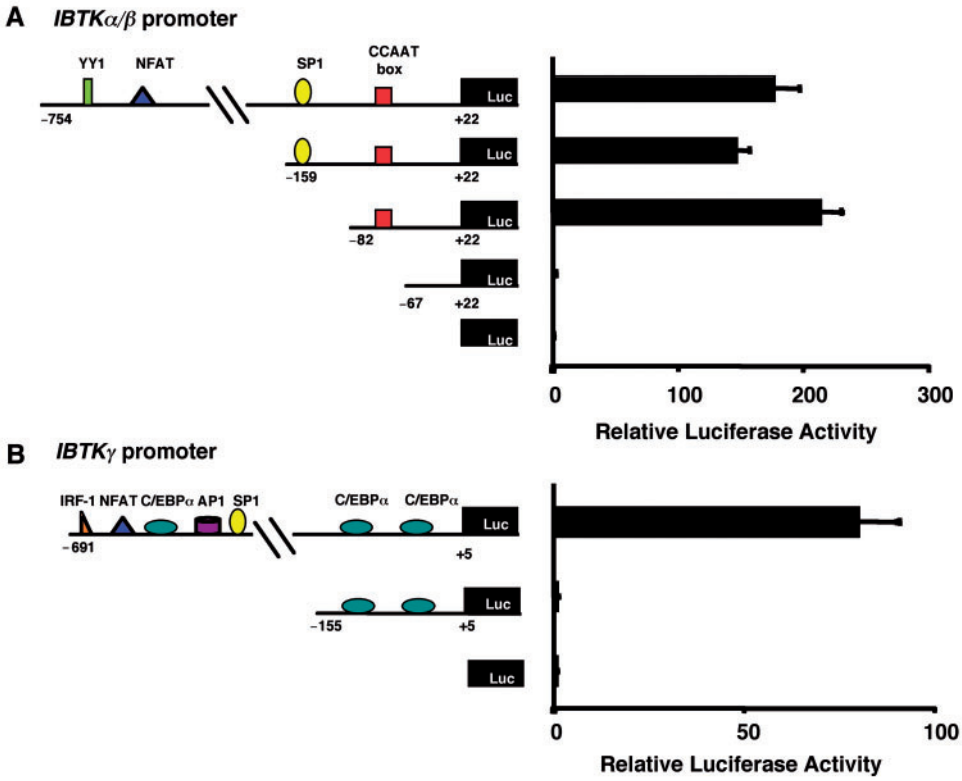

Figure 4. Analysis of *IBTK* promoter regions. Analysis of the *IBTKα*/*IBTKβ* promoter (**A**) and IBTK*γ* promoter (**B**). Human 293T cells were transfected with the indicated *luc* reporter gene constructs. Numbers indicate the positions relative to the first TSS of *IBTK* transcripts (+1). The symbols indicate the presence of promoter regulatory elements of each promoter. The firefly luciferase activity was measured 48 h posttransfection and normalized according to the β-galactosidase activity of the cotransfected plasmid β-Gal. Firefly luciferase activity of reporter gene constructs are shown as fold increase over the pGL3 basic activity. The bars indicate the average of five independent experiments with SEM.

constrained region of IBtk (Figure 3A) and is shared by IBtkα and IBtkα isoforms. Of interest, the ECRi corresponds to the IBtkγ region that binds to the PH domain of Btk (21), suggesting that the ECRi region may function as an evolutionary conserved domain that mediates the physical interactions of IBtk with proteins that carry a PH domain.

Identification and functional characterization of *IBTK* regulatory regions

Next, we undertook a physical and functional analysis of the unknown regulatory regions of the distinct *IBTK* transcripts. To this end, the genomic region spanning from –754 to +22 bp of the *IBTKα*/*β* genes upstream of the TSS were PCR amplified and cloned 5′ to the *luciferase* reporter gene in the pGL3B plasmid, as previously reported (50). This region includes *cis*-regulatory sequences, including CCAAT (nucleotides −75/−70), SP1 (nucleotides −87/−81), NFAT (nucleotides −635/−627) and YY1 (nucleotides −662/−656). In parallel, 5′ deletion mutants were also generated (Figure 4A). Upon transient expression of the *luciferase* reporter gene in 293T cells, we identified a minimal region of −82 + 22 of the *IBTK* gene that regulates the transcription of *IBTKα* and *IBTKβ* transcripts; this region includes a CCAAT *cis* sequence whose deletion abrogates the expression of the *luciferase* reporter gene, indicating that the CCAAT box functions as a major enhancer (Figure 4A). The nucleotide sequence 5′ to the CCAAT box includes additional *cis*-binding sequences for SP1, NFAT and YY1 transcriptional factors; however, these regions did not increase the basal promoter activity of the −82/+22 region (Figure 4A). These results point to CCAAT-binding proteins as major regulators of the *IBTKα*/*β* basal gene transcription.

To identify the regulatory regions responsible for the transcription of *IBTKγ*, a region of 691 bp corresponding to nucleotide –691 to +5 respective to +1 TSS of *IBTKγ* mRNA was PCR amplified and cloned 5′ to the *luciferase* gene in pGL3B plasmid. A sequence analysis of this region (PROSITE) (42) identified an array of potential regulatory *cis*-sequences, such as binding sites for C/EBPα (nucleotides –5/+3; –45/-37), SP1 (nucleotide –210/–200), AP1 (nucleotide –291/–284), C/EBPα (nucleotides –416/–406), NFAT (nucleotides –577/–571), IRF (nucleotides –586/576). As shown in Figure 4B, a significant luciferase activity was observed in 293T cells transfected with the *luciferase* reporter plasmid carrying –691 to +5 nucleotide, while the deletion from –691 to –156 nucleotide abrogated the expression of the *luciferase* reporter gene. These results indicate that the *cis* elements contained within the sequence –691/–156 were required for promoter activity.

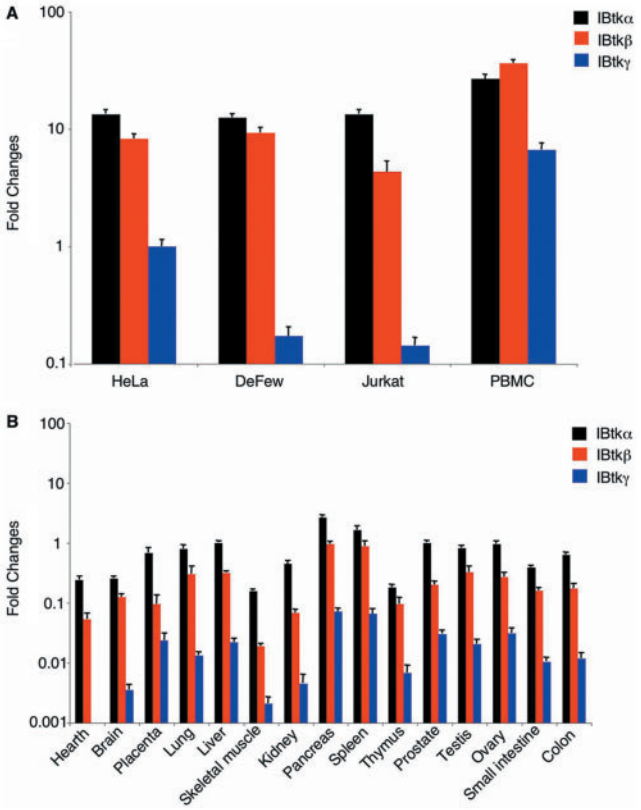

Figure 5. Expression of the *IBTK* mRNAs in human cell lines and tissues.(**A** and **B**) A quantitative expression analysis of the three different *IBTK* mRNAs on HeLa, DeFew, Jurkat, PBMC and a panel of 15 human tissues was performed by real-time PCR. Total RNA was isolated from the distinct cell types and retro-transcribed into cDNA; cDNAs from human tissues were obtained from Clontech. *IBTKα*, *IBTKβ* and *IBTKγ* mRNA were quantified by real-time PCR as described under Materials and methods section. For a comparison among *IBTK* isoforms, the relative expression of *IBTKα* was set equal to 1 in HeLa in the case of cell types, while the expression of liver *IBTKγ* was set equal to 1 in the case of human tissues. The values are reported in a logarithmic scale as the average of three independent experiments and were corrected with a normalization factor considering primers efficiency. The SEM are reported.

Analysis of the *IBTK* expression in a panel of human cell lines and tissues

To assess the expression of the three distinct *IBTKα*, *IBTKβ* and *IBTKγ* transcripts in distinct human cell types, RNAs from the selected cells were reverse transcribed and evaluated by primer-optimized real-time PCR (Figure 5A). The expression of the α, β and γ *IBTK* transcripts was evaluated by using cDNAs from a panel of 15 human tissues (Clontech, shown in Figure 5B). This analysis underscored a differential expression of the three *IBTK* mRNA isoforms, with the general trend showing *IBTKα* as the highest expressed isoform in all the examined cells and tissues, followed by *IBTKβ* and *IBTKγ* (Figure 5A and B).

In vivo detection of IBtk protein isoforms

In vivo detection of IBtkα, IBtkβ and IBtkγ proteins was achieved by using IBtk isoform-specific antibodies. In particular, IBtkα and IBtkβ were detected in cell lysates by using the 31B antibody raised in chicken by immunization with a peptide whose amino acid sequence is divergent in *G. gallus* and is shared by both IBtkα and IBtkβ isoforms (shown in Figure 6A; peptide amino acid sequence is underlined in Figure S1, panels A and B). To overcome the high degree of amino acid sequence homology of the *IBTK* locus among several species, we developed *Ibtk*$^{-/-}$ mice by gene targeting (C. Spatuzza *et al.*, manuscript in preparation), which were immunized with GST-IBtkγ protein. As expected from the *IBtk* gene organization, the mouse anti-GST-IBtkγ serum was specific for IBtkα and IBtkγ proteins, while the anti-31B chicken serum recognized specifically IBtkα and IBtkβ (Figure 6A and B). The three IBtk isoforms were detected in DeFew cells (Figure 6A and B). This analysis was extended in a panel of 293T, HeLa and lymphoid cells (DeFew, Jurkat, MC3 and NB4) (Figure 6C). Further, the expression of IBtk proteins was detected in an array of mouse tissues (Figure 6D); in particular, western blot analysis detected IBtkα and IBtkγ selectively in liver, spleen, thymus and lung; IBtkγ was also expressed in kidney. Both proteins were undetected in brain, cerebellum and heart. Of interest, IBtkγ was expressed at higher levels in spleen and thymus, suggesting a major role in immune regulation (Figure 6D). According to the nucleotide sequence of the mouse *IBtk* locus, the IBtkβ isoform was undetected in the mice tissues (Figure 6D).

To evaluate the specificity of the IBtk antibodies toward the endogenous proteins, we tested the inhibitory activity of a shRNA (clone SH2631H3, Open Biosystems) that targets specifically the *IBTKα* and *IBTKγ* transcripts (Figure S6A). As expected, expression of the SH2631H3 shRNA in Jurkat cells resulted in a drastic reduction of IBtkα and IBtkγ protein isoforms, while the IBtkβ isoform was unaffected (shown in Figure S6B).

Sub-cellular localization of the IBtk isoforms

The localization of the single IBtk isoforms and their *in vivo* association with Btk was analyzed by confocal microscopy as reported (21). In these experiments, the distinct IBtk isoforms were expressed in DeFew B cells and tested for co-localization with endogeneous Btk. As shown in Figure 7, the α and γ isoforms showed a mostly cytoplasmic localization and co-localized with Btk at discrete sub-membrane and cytoplasmic regions (shown in Figure 7, upper and lower panels), consistent with the previous evidence showing that the PH-binding domain of IBtk mediates the physical interaction with Btk (21). Accordingly, the IBtkβ, which showed a nuclear localization, did not colocalize with Btk (Figure 7, middle panels).

In vivo association of IBtk with proteins expressing the PH domain

3The amino acid sequence analysis of the three IBtk isoforms shows that the α and γ isoforms share a domain that mediates a binding with the PH domain of Btk; this domain is missed in the IBtkβ isoform (21); shown in Figure 3A and S1A–C). This evidence suggests that the

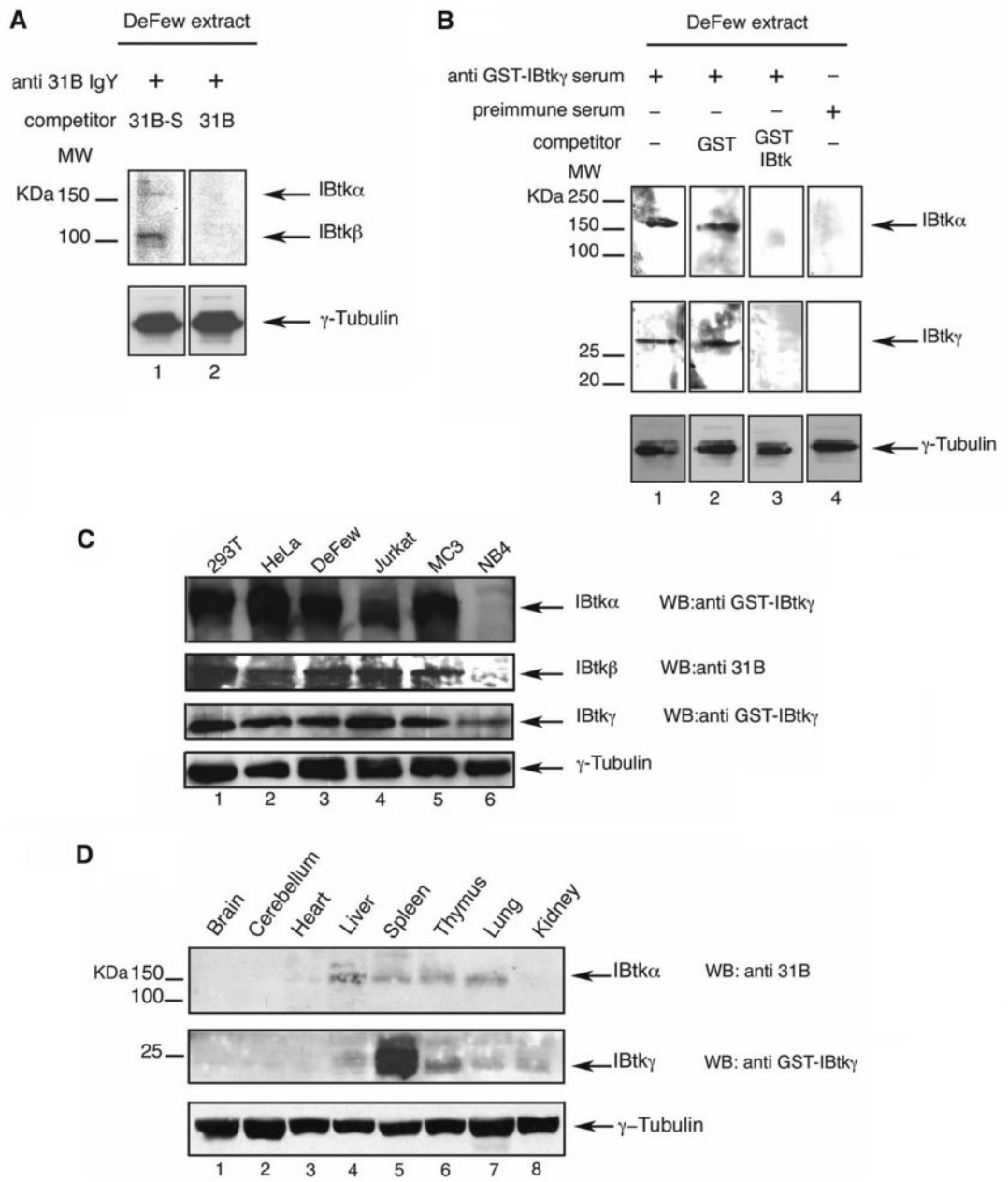

Figure 6. Detection of IBtkα, IBtkβ and IBtkγ endogenous proteins. (**A**) IBtkα (150.53 kDa) and IBtkβ (133.87 kDa) were detected by western blot analysis of DeFew cell extracts (150 μg) by using the anti 31B IgY antibody (10 μg/ml) raised in chickens by using the 31B peptide, which was shared by IBtkα and IBtkβ isoforms. The antibody specificity was assessed by using either the competitor 31B peptide (60 nmoles/ml, lane 2), or a 31B scrambled peptide (60 nmoles/ml, lane 1) in competition experiments. Input proteins were equalized by detecting the endogeneous γ-tubulin. (**B**) IBtkα (150.53 kDa) and IBtkγ (26.31 kDa) were detected by western blot analysis of DeFew cell extracts (100 μg) by using an anti-GST-IBtkγ serum (1:500). The antibody specificities were assessed by using GST (60 nmoles/ml, lane 2), or GST-IBtkγ (60 nmoles/ml, lane 3) proteins in competition experiments. The preimmune serum was unreactive (lane 4). Input proteins were equalized by detecting the endogeneous γ-tubulin. (**C**) Expression of IBtk isoforms. Protein extracts from 293T, HeLa and lymphoblastoid cells (DeFew, Jurkat, MC3, NB4) (50 μg to detect IBtkα and IBtkβ; 100 μg to detect IBtkγ) were tested in western blots by using the indicated antibodies. Input proteins were equalized by detecting the endogeneous γ-tubulin. (**D**) Expression of IBtkα and Ibtkγ in mouse tissues. Western blot analysis was performed by testing 50 μg of protein extracts from mouse tissues. To detect IBtkγ, we used anti GST-IBtkγ serum as primary antibody. IBtkα was detected by the anti-31B IgY. Consistent with the gene organization of mouse *Ibtk*, the mouse IBtkβ isoform was not detected. ECL Plus was performed to detect human IBtkγ.

α and β IBtk isoforms may bind to the PH domain of multiple proteins (http://scop.mrc-lmb.cam.ac.uk/scop-1.69/data/scop.b.c.ib.b.b.html). To test this possibility, a panel of antibodies specific for Btk, Itk (51), Akt1 (52) and PLCγ1 (53), which harbor a PH domain, were used to immune precipitate endogenous IBtk isoforms from primary PBMCs. As reported in Figure 8, IBtkα was detected by western blot by using the specific 31B antibody; in the same setting, the 31B antibody failed to detect the IBtkβ isoform, indicating the IBtkβ does not interact

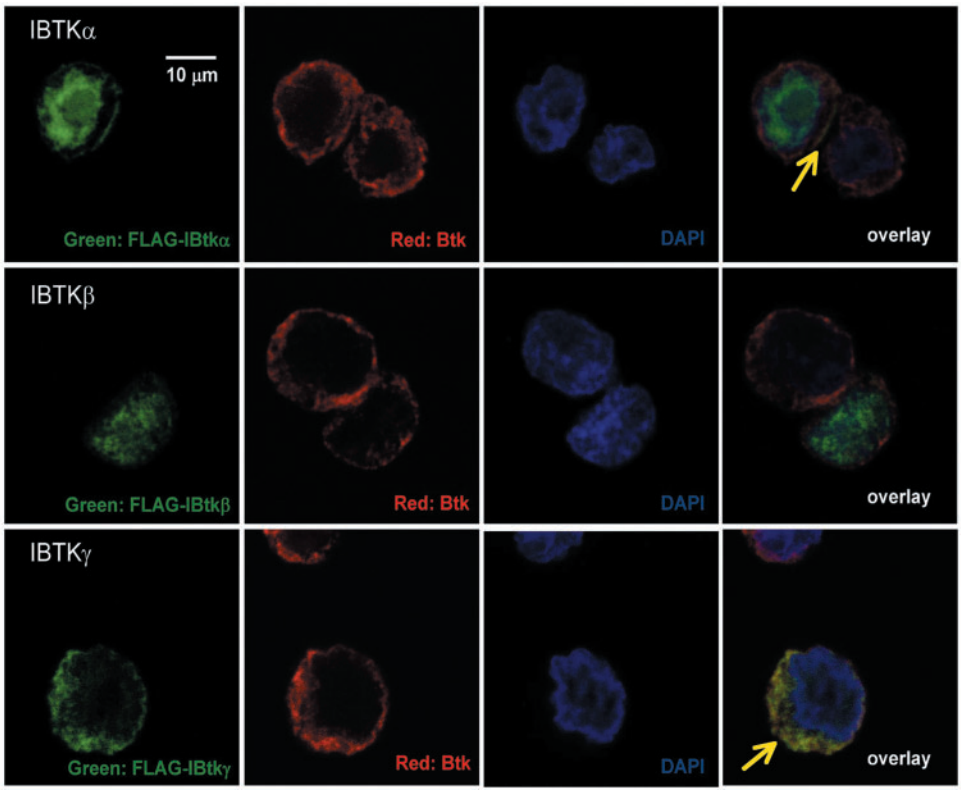

Figure 7. Intracellular localization of Btk and IBtk isoforms in DeFewB lymphoma cells. DeFew cells were transiently transfected with plasmids coding for the three isoforms of IBtk (α, β and γ) fused to FLAG tag. Twenty-four hours later, the cells were fixed and stained with FITC-conjugated anti-FLAG Ab (Green) and anti-Btk Ab, followed by Alexa-568 secondary Ab (Red) and DAPI to detect nuclear DNA. In each panel, a single plane confocal image shows the center of a transfected cell.

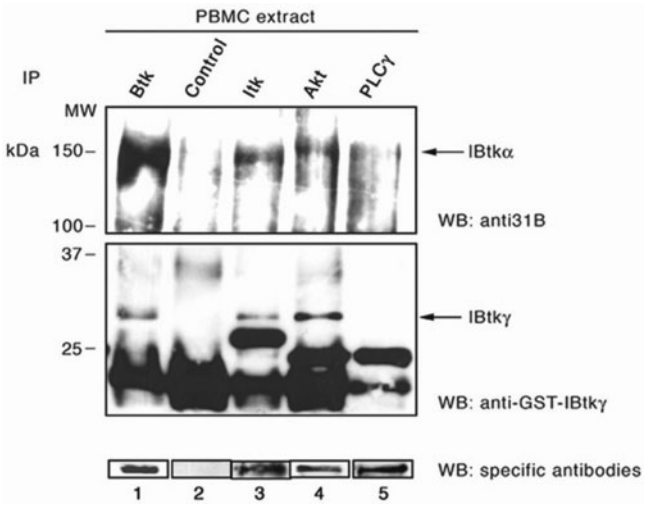

Figure 8. Physical interaction of IBtk with Btk, Itk, Akt and PLCγ1. The *in vivo* presence of protein complexes of the distinct IBtk isoforms with Btk, Itk, Akt and PLCγ$_1$ was assessed by sequential immunoprecipitation and western blot analysis. Primary PBMC were subjected to immune precipitation with anti-Btk, anti-Itk, anti-Akt, anti-PLCγ$_1$ and mouse IgG$_1$ control antibody. To detect IBtkα, IBtkβ, IBtkγ, immunoprecipitates were analyzed by western blotting (WB) by using the anti-31B IgY antibody (upper panel) to detect IBtkα and IBtkβ, and the anti-GST-IBtkγ antibody to detect IBtkγ (middle panel). The lower panel shows the expression of the tested proteins as detected by western blotting with the anti-Btk, anti-Itk, anti-Akt and anti- PLCγ$_1$-specific antibodies.

in vivo with the tested proteins (Figure 8, upper panel). The anti-GST-IBtkγ antibody detected the IBtkγ association with the Btk, Itk and Akt kinases (middle panel). Moreover, IBtkγ did not bind to PLCγ1, while IBtkα showed a strong binding with Btk and a weak interaction with PLCγ1, indicating differential binding affinities for the tested proteins. The lower panel shows the cell expression of the tested proteins, as detected by western blots of the single strips from the upper and middle panels, by using the protein-specific antibodies.

DISCUSSION

The role of Btk in B-cell lymphopoiesis is highlighted by the clinical outcomes of XLA patients and *xid* mice, which have impaired Btk kinase function (1,54). In fact, XLA patients and *xid* mice show a defective development of pre-B cells into later B-cell stages and incomplete differentiation of B-cell precursors to pre-B cells (25). Patients with XLA show heterogeneity in *BTK* gene mutations, including deletions, insertions and substitutions (1,4,6). Mutations occurring in the kinase domain as well as the PH, SH3 or SH2 domains, can induce variable degrees of immunodeficiency (5,24). Thus, distinct regions of Btk are critical for its function in B cells, suggesting that Btk interacts physically with multiple cellular proteins. In fact, the Btk-PH domain binds to both the Ca^{2+}-dependent (α, βI and βII) and Ca^{2+}-independent isoforms (ε and ζ) of PKC

in mouse mast cells and B cells (55,56); to IP_3 (57,58); to βγ as well as Gα12 subunits of heterotrimeric G proteins and to BAP-135 in B cells. Both G12 and BAP-135 function as positive regulators of Btk activity and do not account for the negative regulatory mechanisms required for proper Btk function. In this setting, we have previously identified IBtk as a Btk-PHBM-binding protein that effectively downregulates the Btk tyrosine kinase activity (21). Indeed, IBtkγ binds to the Btk PH domain and promotes a conformational change in Btk, leading to inefficient phosphorylation of Tyr^{223} and reduction of Btk kinase activity by *trans*-inhibitory mechanisms (21,59). Upon binding to Btk, IBtkγ regulates early events in B-cell activation, such as $[Ca^{2+}]_i$ fluxes, and ultimately regulates the gene transcription program mediated by Btk upon BCR cross-linking. IBtk could play a crucial role in the *in vivo* regulation of Btk-mediated B-cell function. In this regard, further study of regulators of Btk, such as IBtk, may lead to a better understanding of the clinical heterogeneity in XLA syndromes characterized by genetic mutations in the Btk-PH domain. To this end, we undertook a comprehensive analysis of the genomic organization of the human *IBTK* locus. Here, we provide the first detailed characterization of *IBTK* as follows: (i) human *IBTK* spans over 77.58 kb and include 29 exons that give raise to three distinct *IBTK* mRNAs; (ii) a fully spliced *IBTKα* mRNA of 5798 nt coding for a protein of 1353 amino acid with a predicted MW of 150.53 kDa; (iii) a second *IBTKβ* mRNA of 4437 nt that ends at a polyadenylation site within intron 24. The *IBTKβ* mRNA includes an ORF coding for a protein of 1196 amino acids with an expected MW of 133.87 kDa. Of interest, the mouse *Ibtk* ortholog does not show a polyadenylation signal within intron 24, indicating that IBtkβ protein is not produced in mice. In this regard, a phylogenetic comparative analysis of the human *IBTK* locus with dog, mouse, chicken, Xenopus, Fugu and Tetradon orthologs indicates that IBtkβ is recently evolved in the human genome, suggesting a distinct role for the IBtkβ isoform (41); (iv) a third human *IBTKγ* mRNA results from a TSS within the intron 24 of the *IBTK* gene and extends over 2328 nt with a ORF coding for a protein of 240 amino acids with an expected 26.31 kDa MW. Of interest, the mouse *Ibtk* ortholog utilizes an ATG TSS within exon 25, with a predicted mouse Ibtkγ isoform of 193 amino acids with a MW of 20.95 kDa.

The three *IBTK* transcripts are regulated by two distinct promoter regions that utilize specific *cis*-regulatory sequences. Indeed, the upstream promoter region (nucleotide −754 to +22 from the +1 TSS) regulates the expression of *IBTKα* and *IBTKβ* transcripts by using the CCAAT box (Figure 4A), which binds preferentially to CAAT-enhancer binding proteins that are shared by most tissues and epithelial cell types (60,61). The transcription expression of *IBTKγ* is regulated by a complex array of IRF-1, NFAT (62,63), CEBPα, AP1 and SP1 transcription factors that binds to the cognate *cis* sequences located at a region spanning from nucleotides −691 to +5 from the +1 nucleotide of the *IBTKγ* (Figure 4B). This complex promoter organization is expected to be restricted to few cell types, such as immune regulatory cells that require a fine-tuned regulation of gene transcription (62). Consistent with the *IBTK* promoter organization, the real-time PCR analysis of an array of human cell lines and tissues, underscored a differential expression of the three *IBTK* transcripts, with *IBTKα* transcripts showing the highest expression in most of the examined cells and tissues (Figure 5).

Western blot analysis detected the distinct IBtkα, and IBtkγ protein isoforms in human and mice cells. According to the bioinformatics analysis and as confirmed by nucleotide sequencing, the IBtkβ isoform was detected in human cells and undetectable in mice tissues (Figure 6). Of interest, the IBtkγ isoform was highly expressed in human lymphoid cells and in mouse spleen cells pointing to a major role of IBtkγ in immune regulation; this possibility is further supported by a first analysis of $Ibtk^{-/-}$ mice that show abnormal proliferation and activation and lymphoid B cells (C. Spatuzza *et al.*, manuscript in preparation). The specificity of the anti-IBtk antibodies was assessed by transducing Jurkat cells either with empty retroviral particles, or with retroviral particles expressing a shRNA sequence specific for the *IBTKα* and *IBTKγ* transcripts. Consistent with the *IBTK* locus organization, a significant decrease of the α and γ IBtk isoforms was observed in shRNA transduced cells; as expected, the expression of IBtkβ protein was unaffected by the shRNA expression (shown in Figure S6).

The resulting IBtkα, IBtkβ and IBtkγ protein isoforms are evolutionarily conserved across vertebrates and include ECR including (i) regulator of chromosome condensation 1 (RCC1) (46,47,64) and BTB(POZ) domains that plays a role in chromatin organization and epigenetic regulation of gene expression (48,49,65); (ii) and ankyrin repeats, which mediate protein–protein interactions (44,45). In addition, the computational analysis has shown a conserved domain (aa 1286–1320 of IBtk, aa 173–207 of IBtkγ) with the highest relative score located at the carboxyl terminus; this region mediates the IBtkγ interaction with the PH domain of Btk (66).

To address the issue of the cell colocalization of the distinct IBtk isoforms, DeFew B lymphoma cells were transduced with plasmid expressing either the α, β or the γ IBtk isoform as FLAG-tag proteins. Cells were stained with anti-FLAG and anti-Btk antibodies and analyzed by confocal microscopy (Figure 7). This analysis underscored a restricted cytoplasmic localization of the IBtkγ isoform; the IBtkα isoform showed a strong cytoplasmic localization and detectable levels of nuclear expression, while IBtkβ showed a restricted nuclear localization. The merging of the IBtk and Btk stainings revealed a colocalization of IBtkα and IBtkγ with Btk; consistent with the lack of a PH-binding domain, IBtkβ was not associated with Btk. These results indicate that IBtkα and IBtkβ, which harbor the RCC1 and BTB/POZ domains, have diverged for the γ isoforms to exert distinct functions as nuclear proteins.

As PH domains are shared by several proteins involved in intracellular signal transductions (67,68), IBtk isoforms may bind to additional proteins and may play a regulatory role beyond the Btk-mediated signal transduction.

This possibility was tested by protein–protein interaction experiments in primary PBMC, where the three distinct IBtk isoforms were tested for *in vivo* binding to Btk, Itk (51), Akt (52) and PLCγ1 (53) proteins. As shown in Figure 8, IBtkα and IBtk γ isoforms showed a distinct association with the tested proteins; as expected from the amino acid sequence of IBtkβ, which lacks the PH-binding domain (Figures 3 and S1B), no binding with the PH domain of the tested proteins was observed in the case of IBtkβ.

SUPPLEMENTARY DATA

Supplementary Data are available at NAR Online.

ACKNOWLEDGEMENTS

We are grateful to Dr P. Schwartzberg, NHGRI-NIH for helping in generating the *Ibtk*$^{-/-}$ mice, Dr N. Zambrano for the *IBTK* siRNA clone. We thank Dr M. Rocchi, Institute of Biomedical Biotechnologies-CNR, 70100 Bari, Italy, for providing the genomic DNA of *Pongo pygmaeus* and *Pan troglodytes*. This work was supported by grants from the Associazione Italiana per la Ricerca sul Cancro (AIRC), MIUR-PRIN, MIUR-FIRB, ISS to G.S. Funding to pay the Open Access publication charges for this article was provided by Department of Experimental and Clinical Medicine, University of Catanzaro, Italy.

Conflict of interest statement. None declared.

REFERENCES

1. Tsukada,S., Rawlings,D.J. and Witte,O.N. (1994) Role of Bruton's tyrosine kinase in immunodeficiency. *Curr. Opin. Immunol.*, **6**, 623–630.
2. Berg,L.J., Finkelstein,L.D., Lucas,J.A. and Schwartzberg,P.L. (2005) Tec family kinases in T lymphocyte development and function. *Annu. Rev. Immunol.*, **23**, 549–600.
3. Broussard,C., Fleischacker,C., Horai,R., Chetana,M., Venegas,A.M., Sharp,L.L., Hedrick,S.M., Fowlkes,B.J. and Schwartzberg,P.L. (2006) Altered development of CD8+ T cell lineages in mice deficient for the Tec kinases Itk and Rlk. *Immunity*, **25**, 93–104.
4. Tsukada,S., Saffran,D.C., Rawlings,D.J., Parolini,O., Allen,R.C., Klisak,I., Sparkes,R.S., Kubagawa,H., Mohandas,T., Quan,S. *et al.* (1993) Deficient expression of a B cell cytoplasmic tyrosine kinase in human X-linked agammaglobulinemia. *Cell*, **72**, 279–290.
5. Lindvall,J.M., Blomberg,K.E., Valiaho,J., Vargas,L., Heinonen,J.E., Berglof,A., Mohamed,A.J., Nore,B.F., Vihinen,M. and Smith,C.I. (2005) Bruton's tyrosine kinase: cell biology, sequence conservation, mutation spectrum, siRNA modifications, and expression profiling. *Immunol. Rev.*, **203**, 200–215.
6. de Weers,M., Mensink,R.G., Kraakman,M.E., Schuurman,R.K. and Hendriks,R.W. (1994) Mutation analysis of the Bruton's tyrosine kinase gene in X-linked agammaglobulinemia: identification of a mutation which affects the same codon as is altered in immunodeficient xid mice. *Hum. Mol. Genet.*, **3**, 161–166.
7. Lee,S.H., Kim,T., Jeong,D., Kim,N. and Choi,Y. (2008) The Tec family tyrosine kinase Btk regulates RANKL-induced osteoclast maturation. *J. Biol. Chem.*, **283**, 11526–11534.
8. Thomas,J.D., Sideras,P., Smith,C.I., Vorechovsky,I., Chapman,V. and Paul,W.E. (1993) Colocalization of X-linked agammaglobulinemia and X-linked immunodeficiency genes. *Science*, **261**, 355–358.
9. Uckun,F.M., Waddick,K.G., Mahajan,S., Jun,X., Takata,M., Bolen,J. and Kurosaki,T. (1996) BTK as a mediator of radiation-induced apoptosis in DT-40 lymphoma B cells. *Science*, **273**, 1096–1100.
10. Scharenberg,A.M. and Kinet,J.P. (1998) PtdIns-3,4,5-P3: a regulatory nexus between tyrosine kinases and sustained calcium signals. *Cell*, **94**, 5–8.
11. Carpenter,C.L. (2004) Btk-dependent regulation of phosphoinositide synthesis. *Biochem. Soc. Trans.*, **32**, 326–329.
12. Petro,J.B., Rahman,S.M., Ballard,D.W. and Khan,W.N. (2000) Bruton's tyrosine kinase is required for activation of IkappaB kinase and nuclear factor kappaB in response to B cell receptor engagement. *J. Exp. Med.*, **191**, 1745–1754.
13. Novina,C.D., Kumar,S., Bajpai,U., Cheriyath,V., Zhang,K., Pillai,S., Wortis,H.H. and Roy,A.L. (1999) Regulation of nuclear localization and transcriptional activity of TFII-I by Bruton's tyrosine kinase. *Mol. Cell Biol.*, **19**, 5014–5024.
14. Shinners,N.P., Carlesso,G., Castro,I., Hoek,K.L., Corn,R.A., Woodland,R.T., Scott,M.L., Wang,D. and Khan,W.N. (2007) Bruton's tyrosine kinase mediates NF-kappa B activation and B cell survival by B cell-activating factor receptor of the TNF-R family. *J. Immunol.*, **179**, 3872–3880.
15. Yu,L., Mohamed,A.J., Simonson,O.E., Vargas,L., Blomberg,K.E., Bjorkstrand,B., Arteaga,H.J., Nore,B.F. and Smith,C.I. (2008) Proteasome dependent auto-regulation of Bruton's tyrosine kinase (Btk) promoter via NF-{kappa}B. *Blood.*, **111**, 4617–4626.
16. Mao,J., Xie,W., Yuan,H., Simon,M.I., Mano,H. and Wu,D. (1998) Tec/Bmx non-receptor tyrosine kinases are involved in regulation of Rho and serum response factor by Galpha12/13. *EMBO J.*, **17**, 5638–5646.
17. Kersseboom,R., Middendorp,S., Dingjan,G.M., Dahlenborg,K., Reth,M., Jumaa,H. and Hendriks,R.W. (2003) Bruton's tyrosine kinase cooperates with the B cell linker protein SLP-65 as a tumor suppressor in Pre-B cells. *J. Exp. Med.*, **198**, 91–98.
18. Jumaa,H., Bossaller,L., Portugal,K., Storch,B., Lotz,M., Flemming,A., Schrappe,M., Postila,V., Riikonen,P., Pelkonen,J. *et al.* (2003) Deficiency of the adaptor SLP-65 in pre-B-cell acute lymphoblastic leukaemia. *Nature*, **423**, 452–456.
19. Hendriks,R.W. and Kersseboom,R. (2006) Involvement of SLP-65 and Btk in tumor suppression and malignant transformation of pre-B cells. *Semin. Immunol.*, **18**, 67–76.
20. Halcomb,K.E., Contreras,C.M., Hinman,R.M., Coursey,T.G., Wright,H.L. and Satterthwaite,A.B. (2007) Btk and phospholipase C gamma 2 can function independently during B cell development. *Eur. J. Immunol.*, **37**, 1033–1042.
21. Liu,W., Quinto,I., Chen,X., Palmieri,C., Rabin,R.L., Schwartz,O.M., Nelson,D.L. and Scala,G. (2001) Direct inhibition of Bruton's tyrosine kinase by IBtk, a Btk-binding protein. *Nat. Immunol.*, **2**, 939–946.
22. Mitelman,F., Mertens,F. and Johansson,B. (1997) A breakpoint map of recurrent chromosomal rearrangements in human neoplasia. *Nat. Genet.*, **15**, 417–474.
23. Inoue,M., Marx,A., Zettl,A., Strobel,P., Muller-Hermelink,H.K. and Starostik,P. (2002) Chromosome 6 suffers frequent and multiple aberrations in thymoma. *Am. J. Pathol.*, **161**, 1507–1513.
24. Dinh,M., Grunberger,D., Ho,H., Tsing,S.Y., Shaw,D., Lee,S., Barnett,J., Hill,R.J., Swinney,D.C. and Bradshaw,J.M. (2007) Activation mechanism and steady state kinetics of Bruton's tyrosine kinase. *J. Biol. Chem.*, **282**, 8768–8776.
25. Contreras,C.M., Halcomb,K.E., Randle,L., Hinman,R.M., Gutierrez,T., Clarke,S.H. and Satterthwaite,A.B. (2007) Btk regulates multiple stages in the development and survival of B-1 cells. *Mol. Immunol.*, **44**, 2719–2728.
26. Sardiello,M., Annunziata,I., Roma,G. and Ballabio,A. (2005) Sulfatases and sulfatase modifying factors: an exclusive and promiscuous relationship. *Hum. Mol. Genet.*, **14**, 3203–3217.
27. Sardiello,M., Licciulli,F., Catalano,D., Attimonelli,M. and Caggese,C. (2003) MitoDrome: a database of Drosophila melanogaster nuclear genes encoding proteins targeted to the mitochondrion. *Nucleic Acids Res.*, **31**, 322–324.
28. Corpet,F. (1988) Multiple sequence alignment with hierarchical clustering. *Nucleic Acids Res.*, **16**, 10881–10890.
29. Simon,A.L., Stone,E.A. and Sidow,A. (2002) Inference of functional regions in proteins by quantification of evolutionary constraints. *Proc. Natl Acad. Sci. USA*, **99**, 2912–2917.
30. Galtier,N., Gouy,M. and Gautier,C. (1996) SEAVIEW and PHYLO_WIN: two graphic tools for sequence alignment and molecular phylogeny. *Comput. Appl. Biosci.*, **12**, 543–548.

31. Yang,Z., Nielsen,R., Goldman,N. and Pedersen,A.M. (2000) Codon-substitution models for heterogeneous selection pressure at amino acid sites. *Genetics*, **155**, 431–449.
32. Korber,B., Muldoon,M., Theiler,J., Gao,F., Gupta,R., Lapedes,A., Hahn,B.H., Wolinsky,S. and Bhattacharya,T. (2000) Timing the ancestor of the HIV-1 pandemic strains. *Science*, **288**, 1789–1796.
33. Burset,M., Seledtsov,I.A. and Solovyev,V.V. (2000) Analysis of canonical and non-canonical splice sites in mammalian genomes. *Nucleic Acids Res.*, **28**, 4364–4375.
34. Stoesser,G., Tuli,M.A., Lopez,R. and Sterk,P. (1999) The EMBL nucleotide sequence database. *Nucleic Acids Res.*, **27**, 18–24.
35. Karolchik,D., Kuhn,R.M., Baertsch,R., Barber,G.P., Clawson,H., Diekhans,M., Giardine,B., Harte,R.A., Hinrichs,A.S., Hsu,F. *et al.* (2008) The UCSC Genome Browser Database: 2008 update. *Nucleic Acids Res.*, **36**, D773–D779.
36. Scala,G., Ruocco,M.R., Ambrosino,C., Mallardo,M., Giordano,V., Baldassarre,F., Dragonetti,E., Quinto,I. and Venuta,S. (1994) The expression of the interleukin 6 gene is induced by the human immunodeficiency virus 1 TAT protein. *J. Exp. Med.*, **179**, 961–971.
37. Livak,K.J. and Schmittgen,T.D. (2001) Analysis of relative gene expression data using real-time quantitative PCR and the 2(-Delta Delta C(T)) method. *Methods*, **25**, 402–408.
38. O'Doherty,U., Swiggard,W.J. and Malim,M.H. (2000) Human immunodeficiency virus type 1 spinoculation enhances infection through virus binding. *J. Virol.*, **74**, 10074–10080.
39. Puca,A., Fiume,G., Palmieri,C., Trimboli,F., Olimpico,F., Scala,G. and Quinto,I. (2007) IkappaB-alpha represses the transcriptional activity of the HIV-1 Tat transactivator by promoting its nuclear export. *J. Biol. Chem.*, **282**, 37146–37157.
40. Mungall,A.J., Palmer,S.A., Sims,S.K., Edwards,C.A., Ashurst,J.L., Wilming,L., Jones,M.C., Horton,R., Hunt,S.E., Scott,C.E. *et al.* (2003) The DNA sequence and analysis of human chromosome 6. *Nature*, **425**, 805–811.
41. Tian,B., Pan,Z. and Lee,J.Y. (2007) Widespread mRNA polyadenylation events in introns indicate dynamic interplay between polyadenylation and splicing. *Genome Res.*, **17**, 156–165.
42. Hulo,N., Sigrist,C.J., Le Saux,V., Langendijk-Genevaux,P.S., Bordoli,L., Gattiker,A., De Castro,E., Bucher,P. and Bairoch,A. (2004) Recent improvements to the PROSITE database. *Nucleic Acids Res.*, **32**, D134–D137.
43. Letunic,I., Copley,R.R., Pils,B., Pinkert,S., Schultz,J. and Bork,P. (2006) SMART 5: domains in the context of genomes and networks. *Nucleic Acids Res.*, **34**, D257–D260.
44. Li,J., Mahajan,A. and Tsai,M.D. (2006) Ankyrin repeat: a unique motif mediating protein-protein interactions. *Biochemistry*, **45**, 15168–15178.
45. Mosavi,L.K., Cammett,T.J., Desrosiers,D.C. and Peng,Z.Y. (2004) The ankyrin repeat as molecular architecture for protein recognition. *Protein Sci.*, **13**, 1435–1448.
46. Khanna,H., Hurd,T.W., Lillo,C., Shu,X., Parapuram,S.K., He,S., Akimoto,M., Wright,A.F., Margolis,B., Williams,D.S. *et al.* (2005) RPGR-ORF15, which is mutated in retinitis pigmentosa, associates with SMC1, SMC3, and microtubule transport proteins. *J. Biol. Chem.*, **280**, 33580–33587.
47. He,S., Parapuram,S.K., Hurd,T.W., Behnam,B., Margolis,B., Swaroop,A. and Khanna,H. (2008) Retinitis pigmentosa GTPase regulator (RPGR) protein isoforms in mammalian retina: insights into X-linked retinitis pigmentosa and associated ciliopathies. *Vision Res.*, **48**, 366–376.
48. Qi,J., Zhang,X., Zhang,H.K., Yang,H.M., Zhou,Y.B. and Han,Z.G. (2006) ZBTB34, a novel human BTB/POZ zinc finger protein, is a potential transcriptional repressor. *Mol. Cell Biochem.*, **290**, 159–167.
49. Xu,J., He,T., Wang,L., Wu,Q., Zhao,E., Wu,M., Dou,T., Ji,C., Gu,S., Yin,K. *et al.* (2004) Molecular cloning and characterization of a novel human BTBD8 gene containing double BTB/POZ domains. *Int. J. Mol. Med*, **13**, 193–197.
50. Ambrosino,C., Palmieri,C., Puca,A., Trimboli,F., Schiavone,M., Olimpico,F., Ruocco,M.R., di Leva,F., Toriello,M., Quinto,I. *et al.* (2002) Physical and functional interaction of HIV-1 Tat with E2F-4, a transcriptional regulator of mammalian cell cycle. *J. Biol. Chem.*, **277**, 31448–31458.
51. Kawakami,Y., Yao,L., Tashiro,M., Gibson,S., Mills,G.B. and Kawakami,T. (1995) Activation and interaction with protein kinase C of a cytoplasmic tyrosine kinase, Itk/Tsk/Emt, on Fc epsilon RI cross-linking on mast cells. *J. Immunol.*, **155**, 3556–3562.
52. Wang,S. and Basson,M.D. (2008) Identification of functional domains in AKT responsible for distinct roles of AKT isoforms in pressure-stimulated cancer cell adhesion. *Exp. Cell Res.*, **314**, 286–296.
53. Suzuki,T., Seth,A. and Rao,R. (2008) Role of phospholipase Cgamma-induced activation of protein kinase Cepsilon (PKCepsilon) and PKCbetaI in epidermal growth factor-mediated protection of tight junctions from acetaldehyde in Caco-2 cell monolayers. *J. Biol. Chem.*, **283**, 3574–3583.
54. Takada,H., Kanegane,H., Nomura,A., Yamamoto,K., Ihara,K., Takahashi,Y., Tsukada,S., Miyawaki,T. and Hara,T. (2004) Female agammaglobulinemia due to the Bruton tyrosine kinase deficiency caused by extremely skewed X-chromosome inactivation. *Blood*, **103**, 185–187.
55. Yao,L., Suzuki,H., Ozawa,K., Deng,J., Lehel,C., Fukamachi,H., Anderson,W.B., Kawakami,Y. and Kawakami,T. (1997) Interactions between protein kinase C and pleckstrin homology domains. Inhibition by phosphatidylinositol 4,5-bisphosphate and phorbol 12-myristate 13-acetate. *J. Biol. Chem.*, **272**, 13033–13039.
56. Venkataraman,C., Chen,X.C., Na,S., Lee,L., Neote,K. and Tan,S.L. (2006) Selective role of PKCbeta enzymatic function in regulating cell survival mediated by B cell antigen receptor cross-linking. *Immunol. Lett.*, **105**, 83–89.
57. Salim,K., Bottomley,M.J., Querfurth,E., Zvelebil,M.J., Gout,I., Scaife,R., Margolis,R.L., Gigg,R., Smith,C.I., Driscoll,P.C. *et al.* (1996) Distinct specificity in the recognition of phosphoinositides by the pleckstrin homology domains of dynamin and Bruton's tyrosine kinase. *EMBO J.*, **15**, 6241–6250.
58. Saito,K., Tolias,K.F., Saci,A., Koon,H.B., Humphries,L.A., Scharenberg,A., Rawlings,D.J., Kinet,J.P. and Carpenter,C.L. (2003) BTK regulates PtdIns-4,5-P2 synthesis: importance for calcium signaling and PI3K activity. *Immunity*, **19**, 669–678.
59. Starr,R., Willson,T.A., Viney,E.M., Murray,L.J., Rayner,J.R., Jenkins,B.J., Gonda,T.J., Alexander,W.S., Metcalf,D., Nicola,N.A. *et al.* (1997) A family of cytokine-inducible inhibitors of signalling. *Nature*, **387**, 917–921.
60. Nicolas,M., Noe,V. and Ciudad,C.J. (2003) Transcriptional regulation of the human Sp1 gene promoter by the specificity protein (Sp) family members nuclear factor Y (NF-Y) and E2F. *Biochem. J.*, **371**, 265–275.
61. Gronostajski,R.M. (2000) Roles of the NFI/CTF gene family in transcription and development. *Gene*, **249**, 31–45.
62. Macian,F. (2005) NFAT proteins: key regulators of T-cell development and function. *Nat. Rev. Immunol.*, **5**, 472–484.
63. de Gorter,D.J., Vos,J.C., Pals,S.T. and Spaargaren,M. (2007) The B cell antigen receptor controls AP-1 and NFAT activity through Ras-mediated activation of Ral. *J. Immunol.*, **178**, 1405–1414.
64. Dasso,M. (1993) RCC1 in the cell cycle: the regulator of chromosome condensation takes on new roles. *Trends Biochem. Sci.*, **18**, 96–101.
65. Bardwell,V.J. and Treisman,R. (1994) The POZ domain: a conserved protein-protein interaction motif. *Genes Dev.*, **8**, 1664–1677.
66. DiNitto,J.P. and Lambright,D.G. (2006) Membrane and juxtamembrane targeting by PH and PTB domains. *Biochim. Biophys. Acta*, **1761**, 850–867.
67. Yao,L., Kawakami,Y. and Kawakami,T. (1994) The pleckstrin homology domain of Bruton tyrosine kinase interacts with protein kinase C. *Proc. Natl Acad. Sci. USA*, **91**, 9175–9179.
68. Kawakami,Y., Yao,L., Han,W. and Kawakami,T. (1996) Tec family protein-tyrosine kinases and pleckstrin homology domains in mast cells. *Immunol. Lett.*, **54**, 113–117.